Coarsening Kinetics of a Spinodally Decomposed Vicinal Si(111) Surface

Yongsam Kim, M. H. Jo, T. C. Kim, C. W. Yang, J. W. Kim, J. S. Hwang, and D. Y. Noh*
Department of Materials Science and Engineering, Center for Extreme Light Applications, Gwangju Institute of Science and Technology, Gwangju, Korea

N. D. Kim and J. W. Chung
Department of Physics, Pohang University of Science and Technology, Pohang, Korea
(Received 17 November 2008; published 17 April 2009)

The coarsening kinetics of the stepped-and-terrace groove structure formed on a vicinal Si(111) surface was investigated by *in-situ* synchrotron x-ray scattering. The time evolution of the groove period L at various temperatures below the (1×1)-to-(7×7) transition falls onto a universal curve when the annealing time is scaled by a scale factor. Distinctive stages of spinodal decomposition, coarsening, and saturation are identified in the evolution of the groove period. L increases following a power law, $L \sim t^n$ with $n = 1/6$ and 0.29 in the initial stage and the late stage of coarsening, respectively. The initial coarsening proceeds via collective motion of step bunches while the late stage is dominated by the diffusion of individual steps.

DOI: 10.1103/PhysRevLett.102.156103 PACS numbers: 68.35.Md, 68.35.Rh, 68.35.bg, 61.05.cm

Self-organized periodic hill-and-valley structures on a silicon surface has attracted renewed attention as templates for the controlled growth of nanostructures [1–3]. Vicinal Si(111) surfaces misoriented towards the $[11\bar{2}]$ direction are particularly interesting since a well-ordered nanoscale hill-and-valley groove structure appears below the (1×1)-to-(7×7) phase transition temperature T_C. As a vicinal Si(111) surface is quenched below T_C, reconstructed (111) terraces appear, which modifies the surface chemical potential leading to the diffusion of adatoms and consequently the step bunching [4–6]. Understanding the kinetic process of the groove formation is necessary to achieve desirable templates by controlling the kinetic variables such as the quench depth and time.

A spinodal line was identified in the temperature-surface orientation phase diagram of the Si(111) surface [4]. Below the spinodal line, a uniformly stepped surface becomes unstable and the phase separates into step-bunched regions and flat terraces with a preferred period. The phase separation is quite analogous to the spinodal decomposition of binary fluid systems. A vicinal Si(111) surface can serve as a model system for the spinodal decomposition on a crystal surface. However, studies [4–8] on the silicon surface are limited to the early stage of decomposition, and do not provide the overall picture of the kinetics involved in the phase separation.

In this Letter, we present an *in-situ* synchrotron x-ray scattering study on the kinetics of a vicinal Si(111) surface quenched into the spinodal decomposition regime focusing on the late stage coarsening. We investigated the evolution of the period L of the stepped-and-terrace groove structure. Four distinctive stages of the step bunching are identified: spinodal decomposition into stepped-and-terrace regions, early stage coarsening, late stage coarsening, and step compaction. Interestingly, the time evolution of L under various quenching temperatures falls onto a universal curve upon scaling the annealing time. During the coarsening, L increases following a power law $\sim t^n$ where n crossovers from $1/6$ to 0.29 as the quenching time increases.

N-type vicinal Si(111) wafers with a 3.5° miscut angle towards $[11\bar{2}]$ were prepared. The sample was flashed at 1430 K by flowing a direct current in the step up direction under a pressure below 5×10^{-10} torr. The clean Si(111) surface was kept above T_C where the surface consists of uniform bilayer steps, and quenched to a desired temperature below the spinodal line. The sample temperature was monitored by an optical pyrometer, which was calibrated by the (1×1)-to-(7×7) transition temperature. The sample temperature during annealing was kept stable within 1 K. For *in-situ* x-ray scattering measurement, samples were mounted in an ultrahigh-vacuum x-ray scattering chamber in the 5C2 beamline at Pohang Light Source (PLS). The incident x-ray beam of 10 keV was monochromatized by a double-bounce Si(111) monochromator which provides $\Delta E/E \approx 2 \times 10^{-4}$. A scintillation one-dimensional point detector was used to detect the diffracted x-rays. The detector resolution determined by slits was 1.7×10^{-3} Å^{-1}.

The x-ray beam was incident on the sample surface in a grazing incident small angle x-ray scattering (GISAXS) geometry [9]. The azimuthal direction of the x-ray beam was parallel to the step-edge x direction. The surface normal direction was set as the z direction, and the step-down direction on the surface was set as the y direction. After a sample was quenched to each desired temperature, the diffraction profile in the y direction was measured repeatedly in *in-situ*. The momentum transfer along Q_z direction was fixed at 0.09 Å^{-1}.

Figure 1(a) shows the time evolution of the GISAXS profiles monitored in real time after the sample was

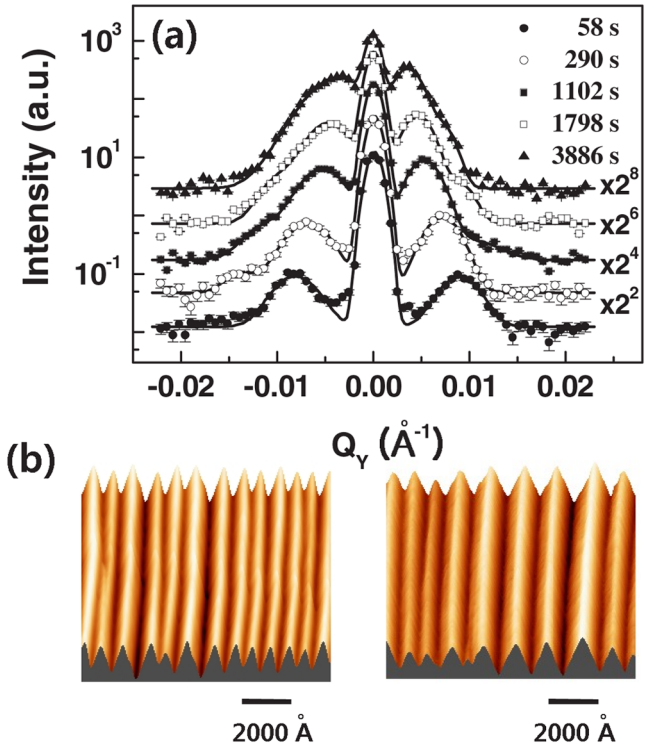

FIG. 1 (color online). (a) Time evolution of x-ray diffraction profiles at $T_C - 35$ K. Solid lines correspond to Gaussian fits. (b) AFM images of the groove structure. (annealing time, left: 900 s and right: 1800 s).

quenched to $T_C - 35$ K. The central peak represents the specular reflection from the average surface. The peaks on the sides are the superlattice reflections which originated from the periodic groove structure illustrated in the *ex-situ* atomic force microscopy (AFM) images in Fig. 1(b). As the quenching time elapses, the superlattice peaks approach the specular peak indicating that the lateral groove period L increases consistent with the AFM images. L is related to the peak position by $L = 2\pi/\Delta Q_y$, where ΔQ_y is the spacing between the specular and the superlattice peak. In addition, the surface became progressively rougher as indicated by the decrease of the specular component. The diffraction profile became asymmetric as the annealing time increased. This was due to the growth of the (111) facets and the stepped bunched area which produced additional scattering features in the sides of the specular peak, respectively. The growth of the facets tilted from the average surface direction was confirmed by the GISAXS profile measured at various Q_z values (data are not shown). The data in Fig. 1(a) are fit to a simple sum of multiple Gaussians since we are interested mainly in the peak position rather than the detailed line shape.

The evolution of L obtained from ΔQ_y at various quenching temperatures is illustrated in Fig. 2(a). At all temperatures, L quickly jumps to above 500 Å in the very early stage of the annealing and coarsens slowly. When the annealing temperature is increased or the quench depth is reduced, the growth of L becomes faster. Most previous

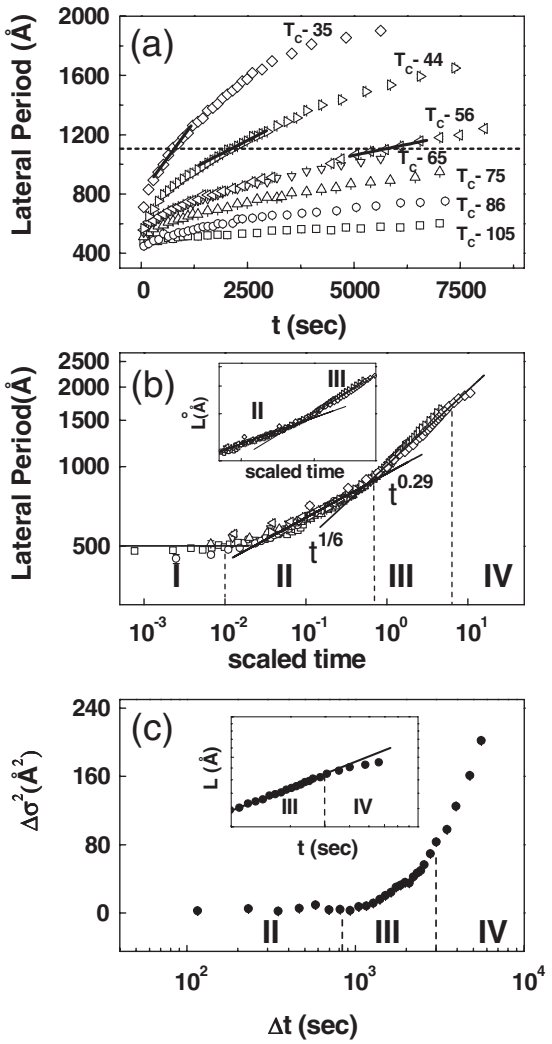

FIG. 2. (a) Growth of the lateral groove period L at several annealing temperatures. Solid lines represent the slopes at $L = 1100$ Å. (b) Evolution of L as a function of the scale time which falls onto a single curve. (c) Surface roughness at $\Delta T = 35$ K. The inset shows the late stage growth of L.

reports were focused on the rather early stage of the phase separation, the spinodal decomposition [4].

The growth of the groove structure period L under various quenching temperatures falls onto a universal curve when the annealing time is divided by an appropriate scale factor $\tau(T)$. For convenience, we chose the scale factor as the time required for L to reach 1000 Å at each temperature. Figure 2(b) shows the period L as a function of the scaled time, $t_s = t/\tau(T)$ in a log-log plot. Remarkably, L falls on a universal curve implying that the coarsening behavior in the temperature range investigated represents common kinetic phenomena. A specific quenching temperature simply determines the speed of the coarsening process and does not alter its nature.

The time dependence of the lateral period L shown in Fig. 2(b) can be divided into four stages. The first stage, region I corresponds to the spinodal decomposition regime

where the groove period reaches an optimum period and stays essentially constant. The coarsening of the groove structure is divided into a slow initial stage (region II), and a fast late stage (region III). The behavior of this two-stage coarsening following a spinodal decomposition is similar to the one observed in a polymer mixture reported by Kuwahara *et al.* [10]. In the final stage, region IV, the coarsening saturates, and step compaction occurs.

The first stage describes the early spinodal decomposition where L jumps to about 500 Å quickly and changes little. If we extrapolate linearly the time dependence of L in the early times at various temperatures, it converges to 500 ± 50 Å as the quenching time approaches zero. The surface decomposes into the 7×7 terraces and the step-bunched regions everywhere simultaneously with a characteristic period of about 500 Å. The existence of the characteristic length is a key feature of a spinodal decomposition. The groove period in this regime is similar to the value reported by Phaneuf *et al.*, 600 Å. All temperatures investigated in this study belong to the spinodal decomposition regime reported by them [4].

In the early stage of the coarsening (region II), the groove period increases slowly following a power-law growth $L \sim t^n$ with a scaling exponent $n = \frac{1}{6}$. As a reference, a line corresponding to the exponent $1/6$ is shown in Fig. 2(b). This coarsening exponent is similar to the value observed in a vicinal Si(113) surface by Song *et al.* [11]. The exponent $1/6$ was theoretically explained by considering the thermal meandering of the step bunches [12]. When the meandering amplitude approaches the groove spacing, two step bunches collide each other and a dislocation is created, which serves as the rate limiting process. The characteristic time τ_M for the meandering is $\sim \Lambda^2/\Gamma M$, where Λ is the typical wavelength of the meandering, Γ and M are the tension and mobility of the step bunch, respectively. Since Λ for the collision is $\simeq \Gamma L^2/k_B T$, and $\Gamma \propto L$, $M \propto 1/L$, τ_M is proportional to L^6, which leads to $L \sim t^{1/6}$. Detailed explanations are given in Ref. [12]. The coarsening proceeds as the dislocation climbs and zips up two step bunches into a single big bunch. The zipping up process is relatively fast. The explanation based on the collective motion of step bunches is plausible since the distance between the grooves is relatively small, and the step bunches have enough mobility in this stage.

The second stage of the coarsening (region III) shown in Fig. 2(b) describes the major coarsening stage with an increased exponent. In this region, L follows a power-law growth as indicated by the linear increase in the log-log scale plot. The coarsening exponent is obtained by fitting L to $L(T, t) = A t_s^n = A[t/\tau(T)]^n$ where $\tau(T)$ is the scale factor and A is a constant. The exponent n thus obtained is 0.29 ± 0.05, which falls in between $1/4$ and $1/3$.

This value of the exponent suggests that the coarsening proceeds by the diffusion of individual steps. Collective motion of the bunches becomes difficult due to the increased stiffness of the bunches as they grow. The tension and mobility of individual steps, however, are independent of the bunch size leading to a larger value of the exponent than the one observed in the initial stage. The exponent $1/4$ was predicted in Mullins' theory of the groove coarsening process where the rate limiting factor is the surface diffusion of atoms [13]. Applying this theory to the steps on the Si surface [14], the coarsening can be understood by the drift of individual steps from a step bunch to the neighbor bunch driven by their chemical potential difference. The change of the terrace width was predicted to scale as $\sim t^{1/4}$ [15].

The increase of the scaling exponent during coarsening has also been reported in a polymer mixture system [10], where initial coarsening exponent $1/6$ was observed and explained by the motion of clusters which is analogous to the collective motion of step bunches. In the later stage, the coarsening crossed over to the Lifshitz-Slyozov process in which individual particles diffuse from small clusters to larger clusters. This results in the diffusion limited ripening with an exponent of $1/3$ [16,17]. $1/3$ or $1/4$ is the expected exponent of a coarsening process with a conserved order parameter. Therefore, we interpret the crossover of the exponent to 0.29 as a signature of the diffusion of individual steps. The coarsening processes of the stage II and III are schematically depicted in Fig. 3. AFM images taken in each stage illustrate the difference in each coarsening stage.

The groove period does not grow indefinitely as illustrated in the inset of Fig. 2(c) that shows the late stage evolution under ΔT of 35 K. The period deviates from the power law at $\sim$3000 s, and starts to saturate. The saturation value of L is determined by the competition between the surface strain energy and the energy cost of forming facet edges [11,18,19].

The surface roughness increases as the groove coarsening progresses. The change of the surface roughness is estimated from the intensity of the specular peak in Fig. 1(a). At a fixed Q_Z, the specular reflectivity $R(Q_Z)$ is

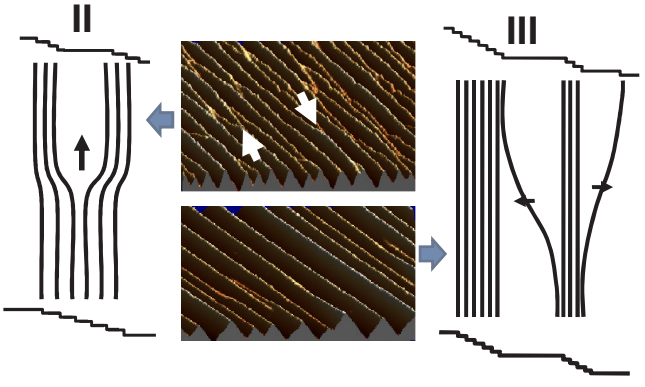

FIG. 3 (color online). Schematic illustration of the coarsening processes II, and III of the groove structures together with corresponding AFM images. White arrows indicates the dislocations.

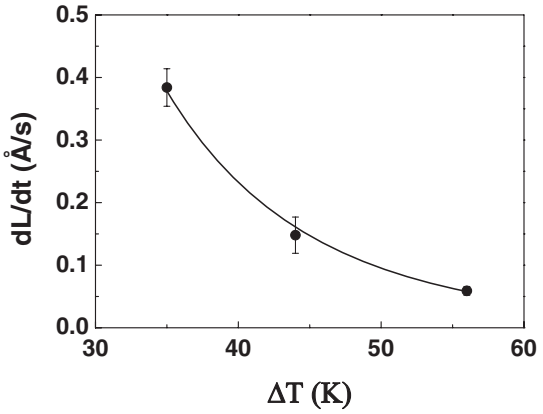

FIG. 4. Coarsening rate, dL/dt as a function of ΔT at $L = 1100$ Å (solid line is a guide to the eye).

given by,

$$R(Q_Z, t) = R_F(Q_Z)e^{-\sigma(t)^2 Q_Z \sqrt{(Q_Z^2 - Q_C^2)}}, \quad (1)$$

where R_F is the Fresnel reflectivity, $\sigma(t)$ is the surface roughness, and Q_C is the wave vector for the total external reflection. The relative change of the square of the roughness, $\Delta\sigma^2 \equiv \sigma(t)^2 - \sigma_0^2$ can be obtained by comparing the specular intensity at time t to that at a reference time t_0. Figure 2(c) shows the evolution of the surface roughness at $\Delta T = 35$ K. During the initial stage region II, there is negligible change in the roughness. This indicates that two step bunches join together at the expense of the terrace in between, and the step-step distance increases. In the stage III, the roughness increases sharply as the groove period L increases. In this stage, the step-step distance decreases as individual step edges move. In the final stage IV, L saturates but the roughness increases. This indicates that the surface morphology keeps changing. The corrugated surface will be stabilized after a long anneal as the angle of the step bunch approaches the value predicted in the equilibrium crystal shape.

The coarsening rate dL/dt increases rapidly as the transition temperature T_C is approached as illustrated by the temperature dependent slopes in Fig. 2(a). By taking a time derivative of $L(t, T)$, one can obtain the coarsening rate. The growth rate at a fixed groove period is inversely proportional to the scale factor, $\tau(T)$. Figure 4 shows the coarsening rate as a function of quench depth, $\Delta T \equiv T_C - T$ obtained at $L = 1100$ Å in the region III. For $\Delta T = 35$ K the coarsening rate is about 6 times larger than for $\Delta T = 56$ K, which cannot be described by an Arrhenius type of a diffusion barrier. This indicates that the mobility of steps is enhanced as the transition temperature is approached. One of the reasons for the change of the rate is that the distance between the steps in the bunched region increases as ΔT decreases. The step mobility is reported to be proportional to the average step distances. A surface with a larger step-step distance is allowed in an equilibrium crystal shape as ΔT is reduced [20].

In summary, the coarsening kinetics of the groove structure on a vicinal Si(111) surface was investigated. During the initial stage, the groove coarsening proceeds by the motion of step bunches, which results in a small coarsening exponent, $\sim 1/6$. As the groove period increases, the coarsening exponent increases to 0.29, which suggests that the diffusion of individual steps dominates.

This work was supported by the Korean Science and Engineering Foundation (KOSEF) through the NRL (M10400000045-04J0000-04510), and NCRC (R15-2008-006-00000-0) grants. J. W. Chung acknowledges the support from the Korea Research Foundation (Grant No. KRF-2006-312-C00513).

*dynoh@gist.ac.kr

[1] C. Gonzalez, P. C. Snijders, J. Ortega, R. Perez, F. Flores, S. Rogge, and H. H. Weitering, Phys. Rev. Lett. **93**, 126106 (2004).
[2] J.-L. Lin, D. Y. Petrovykh, A. Kirakosian, H. Rauscher, and F. J. Himpsel, Appl. Phys. Lett. **78**, 829 (2001).
[3] H. Omi and Y. Homma, Phys. Rev. B **72**, 195322 (2005).
[4] R. J. Phaneuf, N. C. Bartelt, E. D. Williams, W. Swiech, and E. Bauer, Phys. Rev. Lett. **71**, 2284 (1993).
[5] H. C. Jeong and J. D. Weeks, Phys. Rev. Lett. **75**, 4456 (1995).
[6] D.-J. Liu, J. D. Weeks, M. D. Johnson, and E. D. Williams, Phys. Rev. B **55**, 7653 (1997).
[7] N. Israeli, H. C. Jeong, D. Kandel, and J. D. Weeks, Phys. Rev. B **61**, 5698 (2000).
[8] R. J. Phaneuf, N. C. Bartelt, E. D. Williams, W. Swiech, and E. Bauer, Phys. Rev. Lett. **67**, 2986 (1991).
[9] M. Rauscher, R. Paniago, H. Metzger, Z. Kovats, J. Domke, J. Peisl, H. D. Pfannes, J. Schulze, and I. Eisele, J. Appl. Phys. **86**, 6763 (1999).
[10] N. Kuwahara, H. Sato, and K. Kubota, Phys. Rev. E **47**, 1132 (1993).
[11] S. Song, S. G. J. Mochrie, and G. B. Stephenson, Phys. Rev. Lett. **74**, 5240 (1995).
[12] S. Song, M. Yoon, S. G. J. Mochrie, G. B. Stephenson, and S. T. Milner, Surf. Sci. **372**, 37 (1997).
[13] W. W. Mullins, J. Appl. Phys. **28**, 333 (1957).
[14] A. Pimpinelli, J. Villain, D. E. Wolf, J. J. Métois, and J. C. Heyraud, Surf. Sci. **295**, 143 (1993).
[15] N. C. Bartelt, J. L. Goldberg, T. L. Einstein, and E. D. Williams, Surf. Sci. **273**, 252 (1992).
[16] I. M. Lifshitz and V. V. Slyozov, J. Phys. Chem. Solids **19**, 35 (1961).
[17] D. A. Huse, Phys. Rev. B **34**, 7845 (1986).
[18] J. J. Métois, A. Saúl, and P. Müller, Nature Mater. **4**, 238 (2005).
[19] F. K. Men, F. Liu, P. J. Wang, C. H. Chen, D. L. Cheng, J. L. Lin, and F. J. Himpsel, Phys. Rev. Lett. **88**, 096105 (2002).
[20] D. Y. Noh, K. I. Blum, M. J. Ramstad, and R. J. Birgeneau, Phys. Rev. B **44**, 10 969 (1991).